Structure and Dynamics of the α-Lactalbumin Molten Globule: Fluorescence Studies Using Proteins Containing a Single Tryptophan Residue†

Suroopa Chakraborty,‡ Varda Ittah,§ Ping Bai,‡ Li Luo,‡ Elisha Haas,§ and Zheng-yu Peng*,‡

Department of Biochemistry, University of Connecticut Health Center, Farmington, Connecticut 06032, and Department of Life Sciences, Bar Ilan University, Ramat-Gan 52900, Israel

Received January 2, 2001; Revised Manuscript Received April 4, 2001

ABSTRACT: The fluorescence properties of three variants of α-lactalbumin (α-LA) containing a single tryptophan residue were investigated under native, molten globule, and unfolded conditions. These proteins have levels of secondary structure and stability similar to those of the wild type. The fluorescence signal in the native state is dominated by that of W104, with the signal of W60 and W118 significantly quenched by the disulfide bonds in their vicinity. In the molten globule state, the magnitude of the fluorescence signal of W60 and W118 increases, due to the loss of rigid, specific side chain packing. In contrast, the magnitude of the signal of W104 decreases in the molten globule state, perhaps due to the protonation of H107 or quenching by D102 or K108. The solvent accessibilities of individual tryptophan residues were investigated by their fluorescence emission maximum and by acrylamide quenching studies. In the native state, the order of solvent accessibility is as follows: W118 > W60 > W104. This order changes to W60 > W104 > W118 in the molten globule state. Remarkably, the solvent accessibility of W118 in the α-LA molten globule is lower than that in the native state. The dynamic properties of the three tryptophan residues were examined by time-resolved fluorescence anisotropy decay studies. The overall rotation of the molecule can be observed in both the native and molten globule states. In the molten globule state, there is an increase in the extent of local backbone fluctuations with respect to the native state. However, the fluctuation is not sufficient to result in complete motional averaging. The three tryptophan residues in the native and molten globule states have different degrees of motional freedom, reflecting the folding pattern and dynamic heterogeneity of these states. Taken together, these studies provide new insight into the structure and dynamics of the α-LA molten globule, which serves as a prototype for partially folded proteins.

Many proteins adopt a partially folded conformation, termed the molten globule state, under physiological or mildly denaturing conditions (for recent reviews, see refs *1* and *2*; also see refs *3*−*8*). Molten globules have high levels of secondary structure, a compact hydrodynamic radius, and a partially formed, native-like tertiary topology, but they usually do not have rigid, specific side chain packing. Except for proteins that fold via a two-state transition, the molten globule has been proposed to be a general intermediate in protein folding (*9*); thus, studies of molten globules may hold the key to understanding the determinants of protein structure formation in the absence of detailed side chain packing interactions. In addition to their role in protein folding, molten globules may have other biological functions. For example, intrinsically unstructured or partially structured proteins existing under physiological conditions may serve as a conformational switch or target for gene regulation (for a recent review, see ref *10*). Molten globules are involved in a number of biological or pathological processes that require the protein to become partially unfolded, such as interaction with molecular chaperones, translocation across biological membranes, formation of amyloid, and dissociation of supramolecular complexes (*11*−*17*). Finally, point mutations may convert native proteins into molten globule-like species, and some of these mutations correlate with the genetic predisposition for human diseases (*14*, *18*−*22*). Thus, understanding the structure and dynamics of molten globules not only is necessary for understanding the mechanism of protein folding but also may shed light on many natural or disease-related processes.

α-Lactalbumin (α-LA)[1] is a small, two-domain protein, which has been studied extensively as a model system in protein folding (e.g., see refs *23* and *24*). The α-LA molten

† This work was supported by a grant from the National Institutes of Health (1R29-GM54533 to Z.-y.P.) and by a grant from the U.S.-Israel Binational Science Foundation (to E.H. and Z.-y.P.).

* To whom correspondence should be addressed: MC-3305, University of Connecticut Health Center, 263 Farmington Ave., Farmington, CT 06032. Phone: (860) 679-2885. Fax: (860) 679-3408. E-mail: peng@sun.uchc.edu.

‡ University of Connecticut Health Center.

§ Bar Ilan University.

[1] Abbreviations: α-LA, α-lactalbumin; α-LA-W60, α-LA-W104, and α-LA-W118, single-tryptophan-containing α-LAs with W60, W104, and W118, respectively (the other two tryptophan residues were replaced with phenylalanine); HPLC, high-performance liquid chromatography; CD, circular dichroism; NMR, nuclear magnetic resonance; λ_{max}, wavelength of fluorescence emission maximum; λ_{COM}, the center-of-mass wavelength of fluorescence emission spectra; K_{sv}, Stern−Volmer constant; QY, quantum yield; τ_{av}, average fluorescence lifetime; k_q, bimolecular quenching constant; UDP, uridine 5′-diphosphate; GuHCl, guanidine hydrochloride.

10.1021/bi010004w CCC: $20.00
Published on Web 05/23/2001

globule can be observed under a broad range of conditions, including low pH, low concentrations of denaturant, removal of the tightly bound calcium ion, and reduction of disulfide bonds. The similarity between the α-LA molten globule and its kinetic folding intermediate has been established by stopped-flow CD and stopped-flow NMR studies (*25*−*27*). The highly dynamic nature of the α-LA molten globule has precluded the determination of its high-resolution structure by X-ray crystallography or heteronuclear NMR. Although many spectroscopic techniques and disulfide exchange experiments have been used to study the secondary and tertiary structure of the α-LA molten globule, our understanding of the local side chain conformation and dynamics of individual residues is still very limited.

One extremely useful technique for monitoring the local side chain environment and dynamics is tryptophan fluorescence. The intrinsic fluorescence signal of tryptophan has been widely used to follow the kinetics of protein folding (for a recent review, see ref *28*); the solvent accessibility of tryptophan side chains can be estimated by iodide or acrylamide quenching studies (*29*), and the mobility and dynamics of such side chains can be analyzed by time-resolved fluorescence anisotropy decay studies (*30*). In addition, intramolecular distances between a tryptophan and a specifically labeled residue can be measured by fluorescence resonance energy transfer (e.g., see refs *31* and *32*). One potential caveat for these applications is that most proteins contain more than one tryptophan residue; thus, the fluorescence signal is a superposition of signals originating from different tryptophan side chains. This limitation is especially serious for fluorescence anisotropy decay studies, because each tryptophan can potentially produce a decay curve with several exponential time constants. Consequently, a superposition of signals from several tryptophan residues usually cannot be deconvoluted to yield single-residue information (*30*).

In this study, we constructed three variants of α-LA in which two of the three tryptophan residues were replaced with phenylalanine using site-directed mutagenesis. This approach has been used previously to study the cellular retinoic acid binding protein and the RNase inhibitor Barstar (*33*, *34*). The fluorescence properties of these proteins, each containing a single tryptophan residue, were investigated under the native (with or without the bound calcium), the molten globule (pH 2), and the unfolded state, providing information regarding the change in the local side chain environment and mobility for each tryptophan residue as the protein becomes progressively unfolded. These results, in conjunction with previous ^{19}F NMR studies (*35*), have led to a better understanding of the side chain conformation and the time scale of motions in the molten globule state of α-LA.

MATERIALS AND METHODS

Protein Expression and Purification. Recombinant human α-LA and its variant proteins were expressed in *Escherichia coli* as previously described (*36*, *37*). The recombinant α-LA has an additional N-terminal methionine, which reduces its stability in the native state but does not affect its structure or function (*38*−*40*). Site-directed mutagenesis was performed using Kunkel's method (*41*), and the mutations were verified by automated DNA sequencing throughout the entire coding region. Reduced α-LA was refolded by dialysis against a buffer containing 20 mM Tris, 1 mM $CaCl_2$, 2.5 mM cysteine, and 0.5 mM cystine at pH 8.5. The refolded protein was further purified by reverse phase HPLC, lyophilized, and stored at −80 °C. The identity of all proteins was confirmed by electrospray mass spectrometry. The activity of α-LA was determined by measuring the level of stimulation of lactose synthase activity using a coupled enzymatic reaction as described previously (*42*). The specific activity was obtained by plotting the initial rate of UDP production as a function of α-LA concentration.

Circular Dichroism (CD) Spectroscopy. CD studies were performed on a JASCO J-715 spectropolarimeter equipped with a thermoelectric temperature controller. Buffers for the native condition consisted of 10 mM Tris and 1 mM $CaCl_2$ (pH 8.5). Buffers for the molten globule condition consisted of ∼5 mM HCl, and the pH was adjusted to 2.0 with dilute (0.1 M) HCl. The far-UV CD spectra were acquired by using a 1 mm path length cuvette with a 1 nm bandwidth. The near-UV CD spectra were acquired by using a 1 cm path length cuvette with a 5 nm bandwidth. All measurements were conducted at 20 °C. The concentration of the protein was 25 μM for the native condition and 30 μM for the molten globule condition determined by the absorbance at 280 nm in 6 M guanidine hydrochloride (GuHCl), using extinction coefficients of 22 190 M^{-1} cm^{-1} for wild-type α-LA and 10 810 M^{-1} cm^{-1} for variants containing a single tryptophan residue (*43*).

NMR Spectroscopy. One-dimensional proton NMR spectra were acquired using a Varian INOVA plus 600 MHz spectrometer at 20 °C with water suppression by presaturation. The samples consisted of ∼200 μM protein in a 90% H_2O/10% D_2O mixture with 2 mM $CaCl_2$. The pH of the sample was adjusted to 7.0 ± 0.1 with 0.1 M NaOH. The spectra were processed by using Felix.

Fluorescence Spectroscopy. Steady state fluorescence spectra were acquired by using a SPEX Fluorolog spectrofluorimeter at room temperature (23 ± 1 °C). Samples in the native and molten globule states consisted of 1 μM protein in the same buffers used for CD studies. Samples in the unfolded state consisted of 1 μM protein in a buffer containing 10 mM Tris and 8 M urea (pH 8.5). The spectra were recorded using a 1 cm × 1 cm cuvette with an excitation wavelength of 290 or 295 nm and an emission wavelength varying between 310 and 400 nm. Both the excitation and emission slit widths were set to 4 mm. Under these conditions, the optical density of the sample at the excitation wavelength is less than 0.05; thus, the inner filter effect can be neglected (*44*). A sample without protein was used for buffer subtraction. The steady state fluorescence experiments were not conducted under magic angle conditions; thus, the fluorescence spectra, quantum yield, and Stern−Volmer constants could be slightly distorted by the polarization effect. The shapes of the fluorescence spectra obtained at both excitation wavelengths were identical, suggesting that tyrosine does not contribute significantly to the fluorescence intensity. To reduce the day-to-day variation of the instrument, the fluorescence spectra were normalized by the area of a standard tryptophan sample.

Urea Denaturation. Denaturation curves were obtained in the native buffer by measuring the CD signal at 222 nm

($[\Theta]_{222}$) and the center-of-mass wavelength (λ_{COM}) of the fluorescence emission spectra as a function of urea concentration (*45*, *46*). The variables were normalized to yield the fraction of unfolded protein using the following formula

$$f_u = \frac{X - X_u}{X_f - X_u} \quad (1)$$

where X stands for $[\Theta]_{222}$ or λ_{COM} with X_f and X_u representing the values obtained in 0 and 8 M urea, respectively. The midpoint of denaturation was defined as the urea concentration for which f_u equaled 0.5.

Acrylamide Quenching Studies. For each protein in the native, molten globule, and unfolded states, the intensity at the fluorescence emission maximum (λ_{max}) was measured as a function of acrylamide concentration using an excitation wavelength of 290 nm and the same buffer system as described for CD and steady state fluorescence studies. The value of λ_{max} did not change with acrylamide concentration. The fluorescence intensities were corrected for the inner filter effect, and the F_0/F ratio was fit to the Stern−Volmer equation

$$F_0/F = 1 + K_{sv}[Q] \quad (2)$$

where K_{sv} is the Stern−Volmer constant and [Q] is the acrylamide concentration.

Time-Resolved Fluorescence Studies. Time-resolved fluorescence anisotropy decay studies were carried out in four conformational states. Buffers for the native and molten globule states were identical to those described for CD and steady state fluorescence studies. Buffers for the calcium-free apo state consisted of 10 mM Tris and 1 mM EDTA (pH 8.5), and buffers for the unfolded state consisted of 10 mM Tris and 6 M GuHCl (pH 8.5). The samples contained 30 μM protein, and all measurements were carried out at 25 °C. The time-correlated single-photon counting system was described previously (*47*, *48*). The fluorescence decay was monitored at 90° orientation with Glan Thompson polarizers in the path of the excitation and emission beams set at parallel, perpendicular, and magic angle configurations. The system was routinely checked for linearity and time calibration by determination of the decay kinetics of binaphthyl in cyclohexane (decay time is 2.7 ns at 360 nm). Using a 360 nm emission wavelength and a 16 nm slit bandwidth, up to 20 000 counts were recorded for each sample. We used 1024 channels with resolutions of 0.0187 or 0.0374 ns/channel for the long components of the anisotropy decay and 0.005 ns/channel for the short components. The G factor was measured independently for each experiment, and each measurement was repeated three or four times to ensure reproducibility.

Deconvolution and global analysis of the fluorescence decay curves were achieved using the Marquardt, nonlinear least-squares method (*49*). The reference lamp profile used for deconvolution was a scattered light signal generated by a sample containing a suspension of latex beads inside the cell. The decay curves of the magic angle ($I_{54.7°}$), the parallel ($I_{||}$), and the perpendicular ($I_\perp$) configuration were fit to the following equations:

$$I_{54.7°}(t) = \sum_{i=1}^{3} \alpha_i \exp(-t/\tau_i)$$
$$I_{||}(t) = I_{54.7°}[1 + 2r(t)]/3 \quad (3)$$
$$I_\perp(t) = I_{54.7°}[1 - r(t)]/3$$

where $r(t)$ is the anisotropy at time t, which can be expressed as a sum of three exponential functions with rotational correlation times ϕ_i and their initial anisotropy β_i.

$$r(t) = \sum_{i=1}^{3} \beta_i \exp(-t/\phi_i) \quad (4)$$

Using lifetimes τ_i and their relative amplitude α_i from magic angle decay measurements helped us to determine the rotational correlation times and their initial anisotropy by the decays of horizontal and vertical configurations. The best fit was attained by a search for minimal χ^2. The range of uncertainty of the parameters was estimated by a rigorous analysis procedure in which one parameter at a time was fixed at a certain value while all others were floating, thus producing a surface of χ^2 versus the parameter.

Steady state anisotropy data were obtained using an AVIV ATF-105 spectrofluorimeter with excitation and emission wavelengths of 297 and 350 nm, respectively, and slit widths of 1 and 3 nm. Parallel (I_{vv}) and perpendicular (I_{vh}) components were separately measured for the sample as well as for the relevant buffer (B_{vv} and B_{vh}) for background subtraction. The R_{exp} value was an average of 50 points and was calculated with the measured G factor according to

$$R_{exp} = \frac{I_{vv} - B_{vv} - G(I_{vh} - B_{vh})}{I_{tot} - B_{tot}} \quad (5)$$
$$I_{tot} = I_{vv} + 2GI_{vh}$$
$$B_{tot} = B_{vv} + 2GB_{vh}$$

Comparison between the time-resolved and steady state anisotropy values was obtained by calculating R_{calc} from the time-resolved parameters:

$$R_{calc} = 1/\tau_{av} \sum_i \sum_j \alpha_i \beta_j \tau_i \phi_j / (\tau_i + \phi_j) \quad (6)$$
$$\tau_{av} = \sum_{i=1}^{3} \alpha_i \tau_i$$

where τ_{av} is the average lifetime of tryptophan for each protein.

RESULTS

Human α-LA contains three tryptophan residues, which are located at strategic positions in the protein (Figure 1). W60 is sandwiched between the α-helical and β-sheet domain. Since it is believed that the α-helical domain retains a native-like tertiary topology in the α-LA molten globule, whereas the β-sheet domain is significantly unfolded (*50*), W60 may serve as a reporter for the structure reorganization of the β-sheet domain. W104 and W118 are both located inside the α-helical domain and belong to two hydrophobic clusters (*51*, *52*). W104 is located in the hydrophobic box

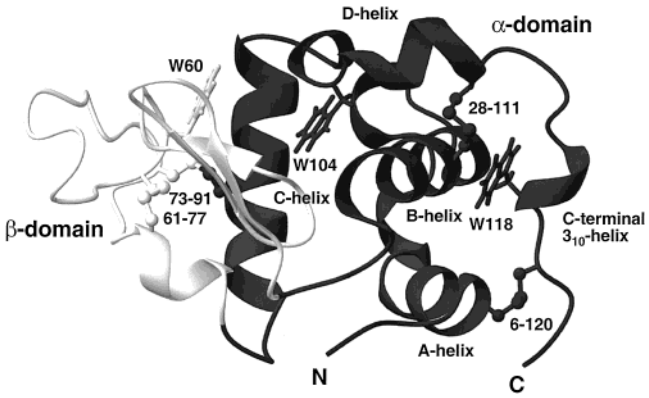

FIGURE 1: Schematic representation of the X-ray crystal structure of human α-LA (*78*), showing the location of three tryptophan side chains. The secondary structure elements and disulfide bonds are labeled. This figure was prepared by using the program MOLMOL (*79*) and PDB entry 1HML.

region surrounded by helices B−D (*53*). Together with M30, F53, W60, I95, I101, and Y103, these residues form hydrophobic cluster II. W118 is located between the B- and C-terminal 3_{10}-helices and is in the vicinity of P24, I27, C28, F31, H32, and Y36. These residues form hydrophobic cluster I. Among residues in these two hydrophobic clusters, I27, Y36, and W118 have been shown previously to be important for the folding and stability of the α-LA molten globule (*54*, *55*).

We produced three variants of α-LA proteins, each containing a single tryptophan residue with the remaining two tryptophan residues replaced with phenylalanine. These proteins are designated as α-LA-W60, α-LA-W104, and α-LA-W118. All three variant proteins refold efficiently to a single-disulfide bond species (data not shown), implying that the substitutions have not compromised the ability of the protein to reach a unique disulfide configuration. The activities of α-LA-W60, α-LA-W104, and α-LA-118 were measured by using a coupled enzymatic assay. α-LA-W104 and α-LA-W118 have 4−5% of the specific activity of the wild type, whereas α-LA-W60 has approximately 12% of the specific activity of the wild type (data not shown).[2] These results were not unexpected because both W104 and W118 are involved in the binding of α-LA with galactosyltransferase and consequently the stimulation of its lactose synthase activity (*52*).

Figure 2 shows the far- and near-UV CD spectra of α-LA-W60, α-LA-W104, and α-LA-W118 in comparison with that of the wild type. Under the native and molten globule conditions, the wild-type α-LA and all three variant proteins have similar values of $[\Theta]_{222}$. Thus, the tryptophan to phenylalanine substitutions have not significantly altered the level of secondary structure. There are, however, some minor differences in the observed far-UV CD spectra (Figure 2A). For example, in the native state, the magnitude of the shoulder near 230 nm is diminished in both α-LA-W104 and α-LA-W118, suggesting that this shoulder is caused by aromatic contributions of W60 to the far-UV CD signal. In the molten globule state, α-LA-W118 appears to have a

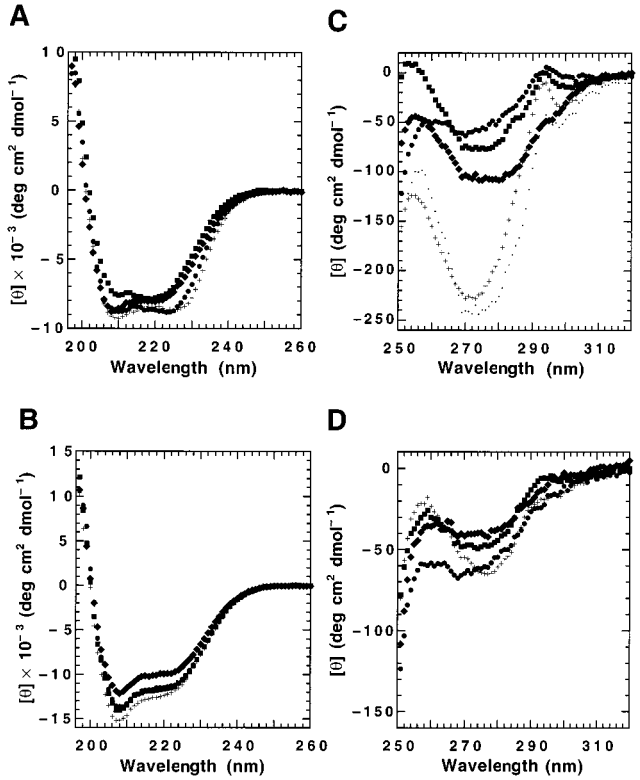

FIGURE 2: Far- and near-UV CD spectra of α-LA-W60 (●), α-LA-W104 (■), and α-LA-W118 (◆) in comparison with that of the wild type (+). (A) Far-UV CD spectra in the native state. (B) Far-UV CD spectra in the molten globule state. (C) Near-UV CD spectra in the native state. (D) Near-UV CD spectra in the molten globule state. In panel C, the sum of three near-UV CD spectra for α-LA-W60, α-LA-W104, and α-LA-W118 is denoted with a dotted line.

slightly lower level of secondary structure than the other three proteins (Figure 2B). Under native conditions, the near-UV CD signal at 270 nm for the three single-tryptophan proteins is less pronounced than that of the wild type (Figure 2C). However, the sum of all three near-UV CD spectra for α-LA-W60, α-LA-W104, and α-LA-W118 is similar to that of the wild type, suggesting that the characteristic peak at 270 nm in wild-type α-LA is made of contributions from individual tryptophan residues. Under molten globule conditions, none of the proteins exhibit a significant near-UV CD signal (Figure 2D), consistent with the loss of rigid, specific side chain packing and with the aromatic residues being in a relatively symmetric environment.

Additional support for the single-tryptophan α-LA having a well-defined tertiary structure comes from one-dimensional NMR studies. At pH 7.0 with 2 mM $CaCl_2$, all three single-tryptophan-containing proteins exhibit proton NMR spectra similar to that of the wild type, including several upfield-shifted methyl groups and a well-dispersed amide region (data not shown), suggesting that no global conformational change has been introduced by mutations.

The fluorescence spectra of the three single-tryptophan variant proteins under the native, molten globule, and unfolded conditions are shown in Figure 3 with the values of λ_{max} listed in Table 1. In the native state, α-LA-W104 exhibits the highest fluorescence intensity, whereas the signals from α-LA-W60 and α-LA-W118 are significantly quenched (Figure 3A). The λ_{max} for α-LA-W104 is 330 nm, characteristic of a buried tryptophan residue. The λ_{max} values

[2] At this time, we do not have an explanation why α-LA-W60, which has both W104 and W118 replaced with phenylalanine, seems to have a slightly higher activity than proteins which have only one of these residues replaced with phenylalanine.

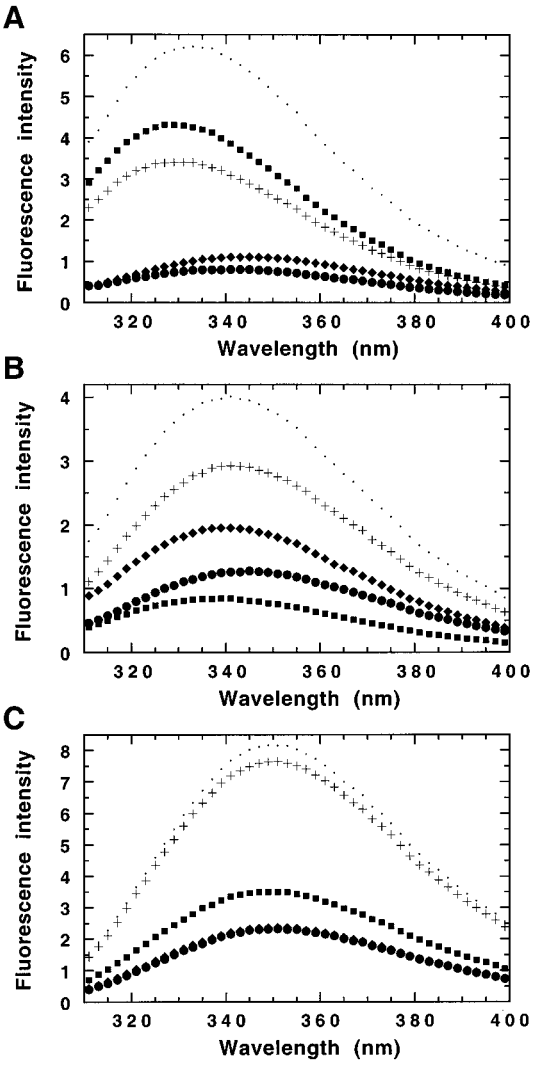

FIGURE 3: Relative fluorescence intensity of α-LA-W60 (●), α-LA-W104 (■), and α-LA-W118 (◆) in comparison with that of the wild type (+). The sum of the spectra of α-LA-W60, α-LA-W104, and α-LA-W118 is denoted with a dotted line. (A) Native state, (B) molten globule state, and (C) unfolded state. All fluorescence intensities were referenced to a tryptophan standard.

Table 1: Fluorescence Emission Maximum (λ_{max}) of α-LA Variants under Different Conditions

	λ_{max} (nm)		
protein	native state (pH 8.5, 1 mM $CaCl_2$)	molten globule state (pH 2)	unfolded state (pH 8.5, 8 M urea)
α-LA-W60	336	344	351
α-LA-W104	330	339	351
α-LA-W118	339	335	351

for α-LA-W60 and α-LA-W118 are slightly red-shifted with respect to that of α-LA-W104, suggesting that the aromatic rings of these residues are partially exposed to the solvent or that the structures surrounding these residues are less rigid. In the molten globule state, the fluorescence intensity of α-LA-W60 and α-LA-W118 increases relative to that of the native state (Figure 3B). Surprisingly, the fluorescence intensity of α-LA-W104, which is the highest in the native state, becomes significantly quenched in the molten globule state. The λ_{max} for α-LA-W60 is shifted from 336 to 344 nm, and the λ_{max} for α-LA-W104 is shifted from 330 to 339 nm, indicating that these residues have gained additional solvent accessibility or became less rigid in the molten globule state. Interestingly, the λ_{max} for α-LA-W118 decreases from 339 to 335 nm, suggesting that this residue is more buried in the molten globule state than in the native state. Although this was a surprising result, the change in solvent accessibility for W118 is fully consistent with that measured by ^{19}F NMR (*35*).

In the unfolded state, all fluorescence spectra have the same λ_{max} values (351 ± 1 nm), suggesting that the tryptophan residues are equally exposed to solvent (Figure 3C). The sum of the fluorescence spectra for α-LA-W60, α-LA-W104, and α-LA-W118 in the unfolded state gives a spectrum that is almost identical to the spectrum of the wild type. This is expected since the tryptophan residues in the unfolded proteins should not interact with each other. In contrast, the sum of the fluorescence spectra for the three single-tryptophan variant proteins in the native and molten globule states has a higher amplitude than the spectrum of the wild type. This is probably due to the existence of energy transfer between different tryptophan residues in the native and molten globule state of the wild-type protein (*56*).

The stability of α-LA-W60, α-LA-W104, and α-LA-W118 was examined by urea denaturation studies in the native buffer (data not shown). As expected for proteins with point mutations, all three single-tryptophan α-LA variants are slightly, but not significantly, less stable than the wild type. We decided to use the transition midpoint, instead of ΔG, to describe the denaturation process, because the denaturation curves monitored by using the center-of-mass wavelength of the fluorescence emission spectra do not superimpose with that monitored by using the far-UV CD signal at 222 nm, suggesting that the transition is not two-state.[3] In general, the denaturation curves monitored by fluorescence have a lower transition midpoint and a higher cooperativity than that monitored by CD, consistent with the change in fluorescence being dominated by the disruption of tertiary structure. On the basis of the fluorescence measurements, all three single-tryptophan proteins have the same stability. The transition midpoint is 3.8 M urea, instead of 4.2 M urea for the wild type. On the basis of the CD measurements, the transition midpoint for α-LA-W118 is essentially the same as that of the wild type (5.2 M), while the transition midpoints for α-LA-W104 and α-LA-W60 are slightly lower, at 4.2 and 4.7 M urea, respectively. Most importantly, all three single-tryptophan variant proteins have a flat baseline between zero and 1.5 M urea, suggesting that these proteins are well-folded under native conditions.

The solvent accessibility of individual tryptophan residues in the native, molten globule, and unfolded states was also investigated by acrylamide quenching studies (Figure 4 and Table 2). The results of these studies are generally in agreement with that of λ_{max}. In the native state, W118 has the highest acrylamide accessibility, as indicated by a Stern−Volmer constant (K_{sv}) that is approximately 30% higher than that of W60 and W104 (Figure 4A). Consistent with that,

[3] When the fluorescence intensities in the native and denatured states are not equal, the center-of-mass wavelength tends to bias toward the state that has a higher fluorescence intensity. However, a more likely explanation for the difference in the two denaturation curves is that the transition is not two-state, since it is known that α-LA adopts a molten globule-like conformation at low denaturant concentrations.

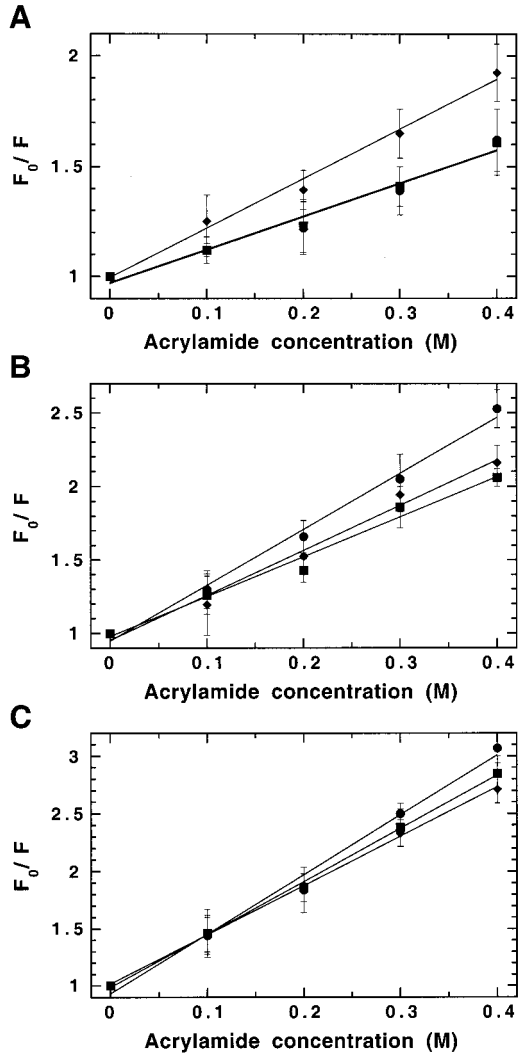

FIGURE 4: Stern−Volmer plots of the acrylamide quenching data for α-LA-W60 (●), α-LA-W104 (■), and α-LA-W118 (◆) in (A) the native state, (B) the molten globule state, and (C) the unfolded state.

Table 2: Stern−Volmer Constants (K_{sv}) Obtained for α-LA Variants under Different Conditions

	K_{sv} (M^{-1})		
protein	native state (pH 8.5, 1 mM $CaCl_2$)	molten globule state (pH 2)	unfolded state (pH 8.5, 8 M urea)
α-LA-W60	1.51 ± 0.08	3.81 ± 0.14	5.23 ± 0.12
α-LA-W104	1.51 ± 0.07	2.72 ± 0.04	4.62 ± 0.17
α-LA-W118	2.25 ± 0.04	1.91 ± 0.09	4.29 ± 0.17

α-LA-W118 also exhibits the most red-shifted fluorescence spectra. The Stern−Volmer constant of W118 decreases upon transition to the molten globule state, whereas those of W60 and W104 increase (Figure 4B). The same trend has also been observed for the change in λ_{max}. In the molten globule state, the order of Stern−Volmer constants for acrylamide quenching is W60 > W104 > W118, consistent with the red shift measured by λ_{max} and solvent-induced isotope shift effect measured by ^{19}F NMR (*35*). On the basis of acrylamide quenching studies, in the unfolded state, there remain some small differences among the three tryptophan residues (Figure 4C). However, these differences have not been confirmed by the values of λ_{max} or by ^{19}F NMR studies.

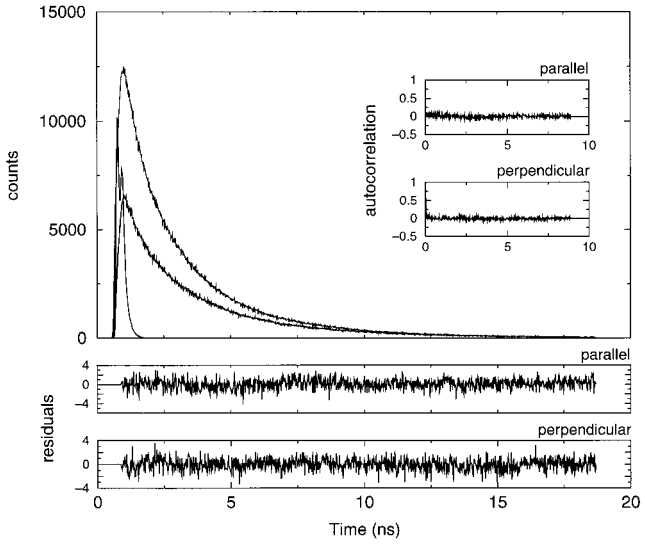

FIGURE 5: Typical fluorescence anisotropy decay curve for α-LA-W104 in the native state. Excitation was at 297 nm, and emission was at 360 nm. The experimental data and lamp profile (peaks near the origin) were fit to eqs 3 and 4 (thin solid lines). The residual χ^2 and the autocorrelation functions are given for both data sets. The best-fit parameters for fluorescence lifetimes and amplitudes are as follows: $\tau_1 = 0.38$, $\alpha_1 = 0.36$, $\tau_2 = 2.04$, $\alpha_2 = 0.51$, $\tau_3 = 4.57$, and $\alpha_3 = 0.13$. The best-fit rotational parameters are listed in Table 3.

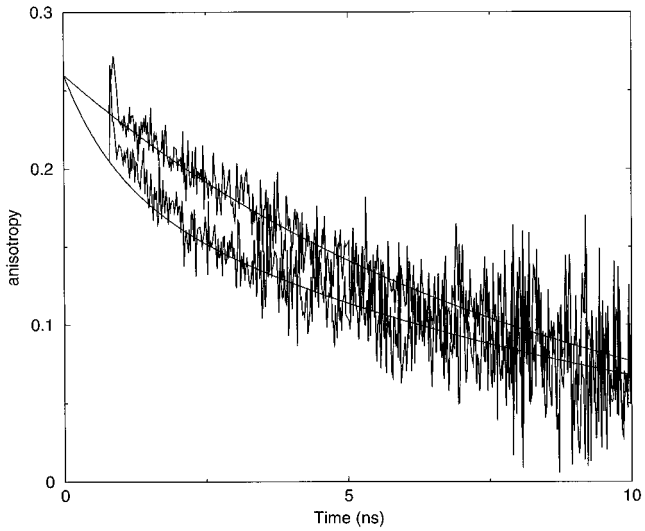

FIGURE 6: Fluorescence anisotropy decays of α-LA-W104 in the native and molten globule states. The best-fit curves are given as thin solid lines, and the parameters are listed in Table 3.

We have investigated the fluorescence anisotropy decay of single-tryptophan α-LA variant proteins in four conformational states: the native, molten globule, unfolded, and apo state (for example, see Figures 5 and 6). The anisotropy decay curves were fit by a sum of exponential functions (up to three), which reflect three different motional relaxation mechanisms (*57*). The fitting parameters are summarized in Table 3. The overall rotation of the molecule has a motional correlation time on the order of 10 ns (*58*); the segmental backbone fluctuation within the molecule typically has a motional correlation time ranging from 1 to 3 ns (*58*, *59*), and the local rotation of the indole side chains has a motional correlation time ranging from 50 to 400 ps. The very fast motions as well as the internal conversion between the ^1L_a and ^1L_b states of tryptophan (*60*, *61*) cannot be resolved by

Table 3: Fitting Parameters for the Time-Resolved Fluorescence Anisotropy Decay Data

protein	τ_{av}[a] (ns)	ϕ_1 (ns) (β_1)[b]	ϕ_2 (ns) (β_2)[b]	ϕ_3 (ns) (β_3)[b]	R_{calc}[c]	R_{exp}[d]	χ^2	QY[e]	τ_{av}/QY	r_{calc}[f] (Å)
α-LA-W60 (native)	1.55	10.6 (0.17)	0.9 (0.06)		0.16	0.21	1.13	0.034	44.9	22.1
α-LA-W60 (molten globule)	1.56	12.0 (0.14)	1.3 (0.11)		0.16	0.17	1.22	0.049	31.5	23.1
α-LA-W60 (unfolded)	1.83		3.5 (0.11)	0.25 (0.12)	0.08	0.13	1.12	0.096	19.2	
α-LA-W60 (apo)	1.78	10.7 (0.18)	1.1 (0.08)		0.17	0.18	1.09			22.2
α-LA-W104 (native)	1.76	8.2 (0.26)			0.20	0.22	1.17	0.151	11.7	20.3
α-LA-W104 (molten globule)	1.48	9.7 (0.19)	0.95 (0.07)		0.17	0.20	1.06	0.035	42.9	21.5
α-LA-W104 (unfolded)	2.21		2.6 (0.15)		0.08	0.16	1.25	0.147	15.0	
α-LA-W104 (apo)	1.97	8.2 (0.21)			0.15	0.17	1.07			20.3
α-LA-W118 (native)	1.58	9.4 (0.16)	1.5 (0.13)		0.18	0.23	1.00	0.053	29.5	21.3
α-LA-W118 (molten globule)	1.53	10.5 (0.15)	2.2 (0.10)		0.18	0.17	1.01	0.079	19.4	22.1
α-LA-W118 (unfolded)	1.87		1.6 (0.16)	0.39 (0.07)	0.10	0.15	1.00	0.098	19.2	
α-LA-W118 (apo)	1.61	10.5 (0.13)	2.0 (0.12)		0.16	0.17	1.06			22.1

[a] The average lifetime calculated by using eq 6. [b] The error in the short and medium ϕ and all β values is ~25%. The error in the long ϕ values is ~40%. [c] The calculated steady state anisotropy according to eq 6. [d] The steady state anisotropy measured by experiment for which the error is at most 20%. [e] Quantum yield, calculated on the basis of the spectra in Figure 3 and a quantum yield value of 0.13 for free tryptophan. [f] The hydrodynamic radius of the protein, calculated with the equation $V = 4\pi r^3/3 = \phi KT/\eta$, where ϕ is the longest rotational correlation time, η is the solvent viscosity; 0.95 cP for aqueous solution and 1.54 cP for 6 M GuHCl solutions at 22 °C. r_{calc} is not a well-defined parameter for the unfolded state.

our system, which has a response time in the range of 50 ps.

The longest motional correlation time observed in the native and molten globule states reflects the overall rotation of the molecule. Interestingly, such motion was not observed in the unfolded state. For each protein, the rotational correlation time in the molten globule state was always slightly longer than that in the native state, consistent with the molten globule having a slightly expanded hydrodynamic radius. The segmental backbone fluctuations of the polypeptide chain, which are on the order of 1−3 ns, were observed in all proteins in the molten globule state, but not always in the native state. α-LA-W104 does not exhibit such motion in the native state, and α-LA-W60 has a smaller contribution of that component in the native state ($\beta = 0.06$) than in molten globule state ($\beta = 0.11$). For α-LA-W118, not much difference was observed between the native and molten globule states. Both forms exhibit comparable contributions from the overall rotation and segmental backbone fluctuation. In the unfolded state, in which the intramolecular interactions are weaker and larger portions of the polypeptide chain are solvated, the protein is expected to adopt a less compact form. This is reflected by an anisotropy decay curve dominated by medium and short components. For example, motions with 1−3 ns correlation times make the most significant contribution to the anisotropy decay of α-LA-W60, α-LA-W104, and α-LA-W118 in the unfolded state ($\beta = 0.11$, 0.15, and 0.16, respectively). Shorter components were also observed in the unfolded state of α-LA-W60 ($\phi = 0.25$ ns, $\beta = 0.12$) and α-LA-W118 ($\phi = 0.39$ ns, $\beta = 0.08$), which probably correspond to the local rotation of tryptophan side chains. Since the 6 M GuHCl solution used to obtain the unfolded state has a viscosity of 1.54 cP at 22 °C while the native buffer has a viscosity of 0.95 cP (*62*), the motional correlation time of the unfolded protein should be divided by 1.6 when it is compared with the motional correlation time of the native protein according to the Stokes−Einstein relationship.

Except for α-LA-W118, the results obtained in the native state are different from the results obtained in the molten globule state, which in turn are different from the results obtained in the unfolded state. The results obtained in the calcium-free apo state are closer to those obtained in the native state than to those of the molten globule state. For α-LA-W118, the properties in the three compact states (the native, molten globule, and apo state) are all similar, perhaps because the location of this residue at a more solvent-exposed position near the end of the polypeptide chain makes the conformational state of the protein having a smaller effect on its mobility.

The steady state anisotropy calculated from the time-resolved data using eq 6, R_{calc}, is generally in reasonable agreement with the steady state anisotropy measured by experiment, R_{exp}, with two exceptions. In the native states of α-LA-W60 and α-LA-W118 and in the unfolded state of the three mutant proteins, the calculated anisotropies from the time-resolved data were lower. This probably is due to an extra weight given to the short anisotropy decay components since the mean fluorescence lifetimes of tryptophan residues are in the range of these components. Thus, the uncertainties of the long anisotropy decay components are larger (α-LA-W104, which does not have a short component, did not show this discrepancy in the native state). In the unfolded state, where the fast anisotropy decay rates dominate the overall decay kinetics, small contributions of a decay component with a correlation time larger than 10 ns may be overlooked by the statistical analysis, and as a result, the calculated steady state anisotropy was reduced.

The intrinsic anisotropy r_0, which should be equal to the sum of all pre-exponential constants β_i, was in the range of 0.21−0.29 for the three tryptophan residues. These values are lower than the fundamental anisotropy of the indole chromophore observed at the same excitation wavelength in a glass state (~0.3) (*63*). Since the internal conversion between the ^1L_a and ^1L_b states has already been taken into account, the reduced values of the intrinsic anisotropy in the present experiments may be due to the limited ability of our system to resolve decay times shorter than 50 ps as well as the underweighting of the contribution of some long components.

DISCUSSION

In this study, we have determined the fluorescence properties of each of the three tryptophan residues in human α-LA. The proteins were investigated under different condi-

tions, covering the native, molten globule, and unfolded states. The fluorescence techniques used here are particularly useful for studying partially folded proteins, since these proteins typically exhibit high levels of side chain mobility and conformational heterogeneity, which prevent structure determination by X-ray crystallography and high-resolution NMR. An additional advantage of the fluorescence technique is that studies can be carried out using relatively dilute protein solutions. This helps avoid aggregation and overcomes the problem of limited solubility often associated with many partially folded proteins.

The fluorescence intensity or quantum yield (QY) of individual tryptophan residues can be used to probe the local environment of these residues. In an earlier study, Sommer and Kronman examined the fluorescence properties of α-LA from four different species (*64*). They estimated the fluorescence quantum yield of individual tryptophan residues by assuming that the fluorescence signals from different tryptophans are independent. Although this procedure gives a reasonable estimate for W28, it leads to a negative quantum yield for W60, which clearly is impossible. Our current data show that the fluorescence intensity of wild-type α-LA is smaller than the sum of intensities for the three single-tryptophan variant proteins (Figure 3), indicating that the additivity relationship does not hold in general for proteins in the native and molten globule states. The differences that we observed could in principle be due to the propagation of conformational changes from the two sites where tryptophan residues were substituted by phenylalanine. More likely, however, this could be due to the energy transfer between individual tryptophan residues in the wild-type protein. In the unfolded state, where subtle conformational changes are eliminated and the distances between tryptophan residues are large, the sum of the fluorescence intensities for the three single-tryptophan-containing proteins is close to that of the wild type.

In the native state, the ratio of the average fluorescence lifetime and the corresponding fluorescence quantum yield for α-LA-W104 is close to the value expected for the radiative lifetime of tryptophan residues (*65*, *66*). For the other two mutant proteins, the τ_{av}/QY ratios were much higher, indicating the presence of static quenching or very fast quenching with a fluorescence lifetime of <50 ps for W60 and W118. Except for W104 in the native state, the other two tryptophan residues in α-LA all have nearby strong quenchers. It is interesting to speculate about which residues or interactions could be responsible for quenching the fluorescence signal. According to the X-ray crystal structure of α-LA, both W60 and W118 are located relatively close to disulfide bonds [cystine is a much stronger quencher than cysteine (*67*)]. Thus, the disulfide bond between residues 61 and 73 potentially is an efficient quencher for W60, and the disulfide bond between residues 6 and 120 potentially is a quencher for W118. In addition, W118 is located close to the disulfide bond between residues 28 and 111 (the distance between W118 and C28 in the native structure is only 3.5 Å). In contrast to W60 and W118, the lack of a short component in the fluorescence anisotropy decay of W104 is consistent with the indole side chain being located in a well-defined, nonquenching environment.

In the molten globule state, the quantum yield of W60 and W118 increases moderately while that of W104 decreases substantially relative to that of the native state. The τ_{av}/QY ratios suggest that both W60 and W104 are significantly quenched, consistent with the existence of an ordered structure with nonlocal contacts. W118 is less quenched in the molten globule state. One likely scenario is that the increase in segmental and side chain mobility probably will reduce the rigidity of interactions between W118 and the putative quenchers, since W118 is three residues apart from the disulfide bond between residues 6 and 120 and the disulfide bond between residues 28 and 111 may be moved away. The increased level of quenching of W104 in the molten globule state suggests that the relaxation of the native structure seems to allow a higher probability of interactions or a closer proximity with quenchers that are restricted in the native state.

Three residues may serve as potential quenchers for W104 in the molten globule state. First, the low-pH condition used to generate the molten globule state will result in protonation of H107, which enhances its ability to quench fluorescence (*67*). Second, D102 and Y103 may also quench the fluorescence of W104, and it has been proposed that in the molten globule state, Y103, W104, and H107 form a non-native cluster (*68*). Evidently, these quenching interactions are either absent or more restricted in the native state.

In the unfolded state, all three tryptophan residues exhibit a relatively high quantum yield and a relatively low but similar τ_{av}/QY ratio. Our results suggest that W60 and W118 may still experience a small amount of static or very fast quenching, perhaps by residues that are located adjacent to or one residue removed from the tryptophan residues in the amino acid sequence. There is no strong evidence suggesting that the structure of the unfolded state deviates significantly from a statistical random coil conformation.

The solvent accessibility of individual tryptophan residues can be inferred from the value of λ_{max} and the value of Stern−Volmer constants obtained in acrylamide quenching studies. Acrylamide has been shown to be an efficient fluorescence quencher, and since it is a neutral molecule, the effect of acrylamide quenching is independent of local charge distributions (*69*). In the native state, the results of our λ_{max} and acrylamide quenching studies are generally in good agreement with the crystal structure of α-LA. For example, the values of λ_{max} for W60, W104, and W118 are 336, 330, and 339 nm, respectively; this order is consistent with the order of solvent accessible surface areas calculated from the X-ray crystal structure (10.4, 5.0, and 17.3 Å^2, respectively). The K_{sv} values for W60, W104, and W118 are 1.51, 1.51, and 2.25 M^{-1}, respectively, also indicating that W118 has the highest solvent accessibility in the native state. The K_{sv} values measured for individual tryptophan residues are comparable with the results for wild-type α-LA (*70*, *71*), although it was surprising that acrylamide quenching cannot distinguish the difference in solvent accessibility between W60 and W104 in the native state. The bimolecular quenching constants (k_q), which can be calculated by dividing K_{sv} with the average fluorescence lifetime, are in the range of $0.8-1.4 \times 10^{-9}$ M^{-1} s^{-1}. Compared to the bimolecular quenching constant of a completely exposed tryptophan [4×10^{-9} M^{-1} s^{-1} (*69*)], these values suggest that the solvent accessibility of tryptophan residues in native α-LA is between 20 and 35%. These values are higher than the solvent accessibility calculated from the crystal structure (on

the basis of the crystal structure, the tryptophan side chains are less than 10% accessible), perhaps because acrylamide may partially penetrate into the interior of the protein. In the molten globule state, W60 becomes the most solvent accessible tryptophan residue, which is likely due to the unfolding of the β-sheet domain. A similar change has also been observed previously in the ^{19}F NMR studies (*35*). On the basis of the fluorescence data, the solvent accessibility of W104 increases moderately upon the transition to the molten globule state. This has not been observed before. However, the ^{19}F NMR and fluorescence studies do not monitor exactly the same property. The fluorescence properties are related to the solvent accessibility of the entire indole ring, whereas the chemical shift values of 5-fluorotryptophan only reflect the local environment of the fluorine atom. Most interestingly, the solvent accessibility of W118 *decreases* upon the transition to the molten globule state. This phenomenon has been observed by ^{19}F NMR, by the change in λ_{max}, and by the change in the Stern−Volmer constant. Thus, we are quite confident that it is not an experimental artifact. These results suggest that in the α-LA molten globule, W118 is located in a buried position. Consistent with this hypothesis, substitutions of W118 significantly lower the effective concentration for formation of the disulfide bond between residues 28 and 111 in the α-LA molten globule as shown by previous studies (*54*, *55*).

On the basis of our fluorescence anisotropy decay studies, the overall dynamic properties of the α-LA molten globule are similar to that of the native state, but are significantly different from that of the unfolded state. In the molten globule state, the long component of the anisotropy decay is maintained, which means that the molecule still retains a globular shape, and the sub-nanosecond motions reflecting the free rotation of side chains are not observed. This is a little surprising because previous NMR studies show that the α-LA molten globule has a narrow range of chemical shift dispersion, presumably due to a dynamic averaging of local side chain conformations (*68*, *72*). NMR relaxation studies and line shape analysis also suggest that the α-LA molten globule is rich in local motions (*35*, *73*). This apparent paradoxical situation can be reconciled by considering the time scale of fluctuation. The fluorescence anisotropy decay occurs on a picosecond to nanosecond time scale, whereas the NMR chemical shift values and line shape are sensitive to motions on a microsecond to millisecond time scale. Thus, one interpretation of these findings is that there is a sufficient amount of tertiary interactions in the α-LA molten globule to suppress fast rotations of side chains present in the unfolded state, but the structure of the molten globule is relaxed to an extent that allows some segmental fluctuations and motions on a time scale that is much longer than the fluorescence lifetime.

The overall rotation of the protein can be analyzed by using the Stokes−Einstein relationship assuming that the shape of the molecule can be approximated as a sphere. Our results (Table 3) show that the equivalent hydrodynamic radii of the protein are in the range of 20−23 Å, with a 5% increase from the native to the molten globule state. These results are in excellent agreement with previous measurements. For example, the effective hydrodynamic radii of α-LA in the native and molten globule states measured by the NMR diffusion method are 19.7 and 20.9 Å, respectively (*74*). The radii of gyration in the native and molten globule states measured by solution state X-ray scattering are 15.7 and 17.2 Å, respectively, which correspond to hydrodynamic radii of 20.3 and 22.2 Å, respectively (*75*). The small differences in hydrodynamic radii between different mutant proteins are probably insignificant, because these values were derived from a 10 ns relaxation time which is considerably longer than the average fluorescence lifetime of tryptophan (the average tryptophan lifetime is ∼1.5 ns; the longest component has a lifetime of ∼5 ns with a relative amplitude of 0.07−0.2).

As expected from the increase in the hydrodynamic radius, there is a small but observable increase in the amplitude of local backbone fluctuations upon the transition from the native to the molten globule state. These motions have a 1−3 ns time scale (*59*, *76*). The increase is more prominent for W104, which has a rigid conformation in the native state, than for W60. For W118, the amplitude of local motions actually decreases in the molten globule state relative to that in the native state, which is consistent with the decrease in solvent accessible surface area. In the native state, the rigidity of the protein is quite different for tryptophan residues located in the different parts of the protein. No local fluctuation was observed for W104, but a significant amount of motion was observed for W118. Although this heterogeneity is smaller in the molten globule state, the region surrounding W104 still seems to have a more rigid structure.

The fast rotation of the tryptophan side chains, which has a correlation time in the range of 50−400 ps (in comparison to 30 ps for free L-tryptophan), does not always exist in native proteins (*59*, *76*, *77*). In our case, no such motion was seen in the native and molten globule states. It is possible that there exists a shorter component, beyond the 50 ps time resolution of our instrument. It is also possible that in the native and molten globule states, the side chain motions are hindered by the compact structure of the protein; thus, a free rotation does not occur on the fluorescence time scale. In the unfolded state, the fast motions of tryptophan side chains can be easily observed for W60 and W118.

Our fluorescence anisotropy decay studies are in good agreement with the λ_{max} and acrylamide quenching studies. W118 has the highest solvent accessibility in the native state, and its anisotropy decay also has the highest contribution from local motions. The solvent accessibility of W118 is more limited in the molten globule state than in the native state and so are the segmental motions ($\beta = 0.1$ instead of 0.13). W60 and W104 are more accessible to the solvent in the molten globule state than in the native state. Consistent with these findings, their anisotropy decay has a higher contribution from local motions in the molten globule state. The unfolded state is the most accessible state for all mutant proteins. The rotational correlation times show the same trend, with more local motions and even the fast rotations of the side chain.

CONCLUSIONS

Analysis of the fluorescence properties of individual tryptophan residues in the α-LA molten globule suggests that the molecule retains a compact, globular shape, and the accessibility, internal quenching, and restricted rotation of side chains can be interpreted by the existence of native-

like tertiary interactions. On the other hand, the structure of the α-LA molten globule is relaxed to an extent to allow the onset of segmental fluctuations and motions slower than the fluorescence lifetime. Our results also confirmed that W118 is buried in a hydrophobic core with a lower solvent accessibility in the molten globule state than in the native state.

ACKNOWLEDGMENT

We thank Ming Li and John Glenn for DNA sequencing, Steve Eyles and Igor Kaltashov for mass spectrometry analysis, Meide Wei and Susan Krueger for assistance in using the fluorescence spectrophotometer, David Friedman for maintenance of the time-resolved fluorescence instrument, and Peter Setlow for careful reading of the manuscript.

REFERENCES

1. Ptitsyn, O. B. (1995) *Adv. Protein Chem. 47*, 83−229.
2. Arai, M., and Kuwajima, K. (2000) *Adv. Protein Chem. 53*, 209−282.
3. Gursky, O., and Atkinson, D. (1996) *Proc. Natl. Acad. Sci. U.S.A. 93*, 2991−2995.
4. Seeley, S. K., Weis, R. M., and Thompson, L. K. (1996) *Biochemistry 35*, 5199−5206.
5. Carroll, A. S., Gilbert, D. E., Liu, X., Cheung, J. W., Michnowicz, J. E., Wagner, G., Ellenberger, T. E., and Blackwell, T. K. (1997) *Genes Dev. 11*, 2227−2238.
6. Zurdo, J., Sanz, J. M., Gonzalez, C., Rico, M., and Ballesta, J. P. (1997) *Biochemistry 36*, 9625−9635.
7. Bychkova, V. E., Dujsekina, A. E., Fantuzzi, A., Ptitsyn, O. B., and Rossi, G. L. (1998) *Folding Des. 3*, 285−291.
8. Zhang, J., and Matthews, C. R. (1998) *Biochemistry 37*, 14881−14890.
9. Ptitsyn, O. B., Pain, R. H., Semisotnov, G. V., Zerovnik, E., and Razgulyaev, O. I. (1990) *FEBS Lett. 262*, 20−24.
10. Wright, P. E., and Dyson, H. J. (1999) *J. Mol. Biol. 293*, 321−331.
11. Flynn, G. C., Beckers, C. J., Baase, W. A., and Dahlquist, F. W. (1993) *Proc. Natl. Acad. Sci. U.S.A. 90*, 10826−10830.
12. Hayer-Hartl, M. K., Ewbank, J. J., Creighton, T. E., and Hartl, F. U. (1994) *EMBO J. 13*, 3192−3202.
13. Robinson, C. V., Grob, M., Eyles, S. J., Ewbank, J. J., Mayhew, M., Hartl, F. U., Dobson, C. M., and Radford, S. E. (1994) *Nature 372*, 646−651.
14. Booth, D. R., Sunde, M., Bellotti, V., Robinson, C. V., Hutchinson, W. L., Fraser, P. E., Howkins, P. N., Dobson, C. M., Radford, S. E., Blake, C. C. F., and Pepys, M. B. (1997) *Nature 385*, 787−793.
15. Ren, J., Kachel, K., Kim, H., Malenbaum, S. E., Collier, R. J., and London, E. (1999) *Science 284*, 955−957.
16. Schwartz, M. P., Huang, S., and Matouschek, A. (1999) *J. Biol. Chem. 274*, 12759−12764.
17. Ramirez-Alvarado, M., Merkel, J. S., and Regan, L. (2000) *Proc. Natl. Acad. Sci. U.S.A. 97*, 8979−8984.
18. Lim, W. A., Farruggio, D. C., and Sauer, R. T. (1992) *Biochemistry 31*, 4324−4333.
19. Zhang, B., and Peng, Z.-y. (1996) *J. Biol. Chem. 271*, 28734−28737.
20. Kelly, J. W., Colon, W., Lai, Z., Lashuel, H. A., McCulloch, J., McCutchen, S. L., Miroy, G. J., and Peterson, S. A. (1997) *Adv. Protein Chem. 50*, 161−181.
21. Yuan, C., Byeon, I.-J. L., Poi, M.-J., and Tsai, M.-D. (1999) *Biochemistry 38*, 2919−2929.
22. Matthews, J. M., Norton, R. S., Hammacher, A., and Simpson, R. J. (2000) *Biochemistry 39*, 1942−1950.
23. Kuwajima, K., Mitani, M., and Sugai, S. (1989) *J. Mol. Biol. 206*, 547−561.
24. Kuwajima, K. (1996) *FASEB J. 10*, 102−109.
25. Ikeguchi, M., Kuwajima, K., Mitani, M., and Sugai, S. (1986) *Biochemistry 25*, 6965−6972.
26. Balbach, J., Forge, V., van Nuland, N. A. J., Winder, S. L., Hore, P. J., and Dobson, D. M. (1995) *Nat. Struct. Biol. 2*, 865−870.
27. Arai, M., and Kuwajima, K. (1996) *Folding Des. 1*, 275−287.
28. Eftink, M. R., and Shastry, M. C. (1997) *Methods Enzymol. 278*, 258−286.
29. Eftink, M. R., and Ghiron, C. A. (1981) *Anal. Biochem. 114*, 199−227.
30. Beechem, J. R., and Brand, L. (1985) *Annu. Rev. Biochem. 54*, 43−71.
31. Rischel, C., Thyberg, P., Rigler, R., and Poulsen, F. M. (1996) *J. Mol. Biol. 257*, 877−885.
32. Chan, C. K., Hu, Y., Takahashi, S., Rousseau, D. L., Eaton, W. A., and Hofrichter, J. (1997) *Proc. Natl. Acad. Sci. U.S.A. 94*, 1779−1784.
33. Clarke, A. R., and Waltho, J. P. (1997) *Curr. Opin. Biotechnol. 8*, 400−410.
34. Swaminathan, R., Nath, U., Udgaonkar, J. B., Periasamy, N., and Krishnamoorthy, G. (1996) *Biochemistry 35*, 9150−9157.
35. Bai, P., Luo, L., and Peng, Z.-y. (2000) *Biochemistry 39*, 372−380.
36. Peng, Z.-y., and Kim, P. S. (1994) *Biochemistry 33*, 2136−2141.
37. Schulman, B. A., Redfield, C., Peng, Z.-y., Dobson, C. M., and Kim, P. S. (1995) *J. Mol. Biol. 253*, 651−657.
38. Chaudhuri, T. K., Horii, K., Yoda, T., Arai, M., Nagata, S., Terada, T. P., Uchiyama, H., Ikura, T., Tsumoto, K., Kataoka, H., Matsushima, M., Kuwajima, K., and Kumagai, I. (1999) *J. Mol. Biol. 285*, 1179−1194.
39. Ishikawa, N., Chiba, T., Chen, L. T., Shimizu, A., Ikeguchi, M., and Sugai, S. (1998) *Protein Eng. 11*, 333−335.
40. Veprintsev, D. B., Narayan, M., Permyakov, S. E., Uversky, V. N., Brooks, C. L., Cherskaya, A. M., Permyakov, E. A., and Berliner, L. J. (1999) *Proteins: Struct., Funct., Genet. 37*, 65−72.
41. Kunkel, T. A., Robert, J. D., and Zakour, R. A. (1987) *Methods Enzymol. 154*, 367−382.
42. Fitzgerald, D. K., Colvin, B., Mawal, R., and Ebner, K. E. (1970) *Anal. Biochem. 36*, 43−61.
43. Edelhoch, H. (1967) *Biochemistry 6*, 1948−1954.
44. Lakowicz, J. R. (1999) *Principles of fluorescence spectroscopy*, 2nd ed., Kluwer Academic/Plenum Publishers, New York.
45. Shao, X., Hensley, P., and Matthews, C. R. (1997) *Biochemistry 36*, 9941−9949.
46. Bilsel, O., Yang, L., Zitzewitz, J. A., Beechem, J. M., and Matthews, C. R. (1999) *Biochemistry 38*, 4177−4187.
47. Gottfried, D. S., and Haas, E. (1992) *Biochemistry 31*, 11353−11362.
48. Ittah, V., and Haas, E. (1995) *Biochemistry 34*, 4493−4506.
49. Beechem, J. M., and Haas, E. (1989) *Biophys. J. 55*, 1225−1236.
50. Wu, L. C., Peng, Z.-y., and Kim, P. S. (1995) *Nat. Struct. Biol. 2*, 281−286.
51. Acharya, K. R., Stuart, D. I., Walker, N. P. C., Lewis, M., and Phillips, D. C. (1989) *J. Mol. Biol. 208*, 99−127.
52. Grobler, J. A., Wang, M., Pike, A. C., and Brew, K. (1994) *J. Biol. Chem. 269*, 5106−5114.
53. Koga, K., and Berliner, L. J. (1985) *Biochemistry 24*, 7257−7262.
54. Song, J., Bai, P., Luo, L., and Peng, Z.-y. (1998) *J. Mol. Biol. 280*, 167−174.
55. Wu, L. C., and Kim, P. S. (1998) *J. Mol. Biol. 280*, 175−182.
56. Clark, P. L., Weston, B. F., and Gierasch, L. M. (1998) *Folding Des. 3*, 401−412.
57. Elofsson, A., Rigler, R., Nilsson, L., Roslund, J., Krause, G., and Holmgren, A. (1991) *Biochemistry 30*, 9648−9656.
58. Tcherkasskaya, O., Ptitsyn, O. B., and Knutson, J. R. (2000) *Biochemistry 39*, 1879−1889.
59. Kemple, M. D., Buckley, P., Yuan, P., and Prendergast, F. G. (1997) *Biochemistry 36*, 1678−1688.

60. Ruggiero, A. J., Todd, D. C., and Fleming, G. R. (1990) *J. Am. Chem. Soc. 112*, 1003−1014.
61. Callis, P. R. (1997) *Methods Enzymol. 278*, 113−150.
62. Kawahara, K., and Tanford, C. (1966) *J. Biol. Chem. 241*, 3228−3232.
63. Valeur, B., and Weber, G. (1977) *Photochem. Photobiol. 25*, 441−444.
64. Sommers, P. B., and Kronman, M. J. (1980) *Biophys. Chem. 11*, 217−232.
65. Kirby, E. P., and Steiner, R. F. (1970) *J. Phys. Chem. 74*, 4480−4490.
66. Petrich, J. W., Chang, M. C., McDonald, D. B., and Fleming, G. R. (1983) *J. Am. Chem. Soc. 105*, 3824−3832.
67. Chen, Y., and Barkley, M. D. (1998) *Biochemistry 37*, 9976−9982.
68. Alexandrescu, A. T., Evans, P. A., Pitkeathly, M., Baum, J., and Dobson, C. M. (1993) *Biochemistry 32*, 1707−1718.
69. Eftink, M. R., and Ghiron, C. A. (1976) *Biochemistry 15*, 672−680.
70. France, R. M., and Grossman, S. H. (2000) *Biochem. Biophys. Res. Commun. 269*, 709−712.
71. Lala, A. K., and Kaul, P. (1992) *J. Biol. Chem. 267*, 19914−19918.
72. Baum, J., Dobson, C. M., Evans, P. A., and Hanley, C. (1989) *Biochemistry 28*, 7−13.
73. Kim, S., Bracken, C., and Baum, J. (1999) *J. Mol. Biol. 294*, 551−560.
74. Redfield, C., Schulman, B. A., Milhollen, M. A., Kim, P. S., and Dobson, C. M. (1999) *Nat. Struct. Biol. 6*, 948−952.
75. Kataoka, M., Kuwajima, K., Tokunaga, F., and Goto, Y. (1997) *Protein Sci. 6*, 422−430.
76. Lakshmikanth, G. S., and Krishnamoorthy (1999) *Biophys. J. 77*, 1100−1106.
77. Kim, Y.-R., Hahn, J.-S., Hong, H., Jeong, W., Song, N. W., Shin, H.-C., and Kim, D. (1999) *Biochim. Biophys. Acta 1429*, 486−495.
78. Acharya, K. R., Ren, J., Stuart, D. I., and Phillips, D. C. (1991) *J. Mol. Biol. 221*, 571−581.
79. Koradi, R., Billeter, M., and Wuthrich, K. (1996) *J. Mol. Graphics 14*, 51−55.

BI010004W